

Excitation mechanism and dynamics of magnetoacoustic oscillations in the earth's bow shock

A. A. Galeev, S. I. Klimov, M. N. Nozdachev, R. S. Sagdeev, and A. Yu. Sokolov

Institute of Space Studies, Academy of Sciences of the USSR

(Submitted 16 December 1985)

Zh. Eksp. Teor. Fiz. **90**, 1690–1700 (May 1986)

A theory is developed for ion-beam excitation of magnetoacoustic oscillations at lower-hybrid frequencies which propagate across the magnetic field in a high- β plasma ($\beta \gtrsim 1$). It is shown that due to strong Landau damping by thermal ions, oscillations are excited in a weakly nonisothermal plasma ($T_e \gtrsim T_i$) at frequencies nearly an order of magnitude lower than the lower-hybrid resonance frequency. At these frequencies it is important to take into account the work done by the beam ions in the solenoidal electric field of the oscillations. Measurements of the oscillation spectrum recorded by the "Prognoz-10-Interkosmos" satellite are discussed. The measured growth rate of the oscillations, the position of the spectral energy density maximum, and the time behavior of the spectrum agree closely with the theoretical growth rate and frequency for the fastest-growing oscillations, provided one assumes the oscillations are excited by a beam of ions reflected from the shock wave front.

INTRODUCTION

The launching of man-made satellites into earth orbit has transformed space into a natural plasma laboratory in which plasma diagnostics can be carried out much more thoroughly than is possible in earth-bound laboratories. In particular, experiments in space are now stimulating considerable progress in collisionless shock wave studies. Most of the experimental data here have been obtained from measurements at the wavefront of the bow shock wave which is continuously generated ahead of the earth as it passes through the solar wind, the supersonic stream of plasma from the solar corona. The fundamental problem here is to identify the collisionless mechanisms by which the kinetic energy of the plasma flux is dissipated at the shock front. It is now firmly established¹ that for shocks propagating across a magnetic field, much of the energy of the plasma stream goes to accelerate a relatively large number ($<25\%$) of the ions in the plasma which then escape into the region ahead of the front. In the magnetohydrodynamic (MHD) description, the escape of these ions in the forward direction is attributed to "overturning" of the plasma velocity profile at the shock wave front.² It was also suggested² that the energy of the forward ions should be dissipated through the excitation of a two-stream instability by ions moving transverse to the magnetic field at frequencies close to the low-hybrid resonance frequency. However, breaking of the hydrodynamic plasma velocity profile is not meaningful in a more rigorous kinetic description of the plasma; instead, one must analyze how the ions in the incident plasma stream are reflected by the retarding electrostatic field at the wavefront and by the Lorentz force (induced field) which is generated when the plasma stream is deflected in the self-consistent electric field of the ions reflected or transmitted across the front.³ Analysis shows that the reflected ions gain additional energy in the self-consistent induced field $E = -u \times B / c$ (here E and B are the electric and magnetic field vectors, and u is the hy-

drodynamic velocity of the plasma). In other words, a substantial portion of the plasma kinetic energy is first transferred to the reflected ions and is only then converted into other forms of energy (plasma heating, kinetic energy of accelerated particles, etc.) through the growth of instability in the reflected ion beam in the plasma. It is thus clear that for fast shocks ($M \gg 1$), the amount of energy conversion is much greater than occurs in collective processes associated with gradients in the magnetic field and in the plasma density and temperature. This is because the magnetic field and the thermal motion of the plasma contain much less energy than the beam of reflected ions.

It is well-established that the reflected ion beam thermalizes, and much is known concerning the relaxation process (see, e.g., Ref. 4); however, it remains unclear which plasma modes are preferentially excited by the beam and responsible for its relaxation. The most likely candidates are the lower-hybrid oscillations excited by ion beams counterstreaming in a magnetic field.² The earliest plasma wave measurements at lower-hybrid frequencies⁵ carried out on the "Prognoz-8" satellite showed that lower-hybrid oscillations are always present at strong shock wave fronts, and it was suggested⁵ that they are generated by a beam of reflected ions. However, no detailed theoretical analysis has yet been given for how these oscillations are excited by ion beams moving in opposite directions in plasmas with finite β_i and β_e ($\beta_j = 8\pi n T_j / B^2$, $j = i$ or e , is the pressure of plasma component j divided by the magnetic pressure, where T_j is measured in energy units). This is because in contrast to the low- β case, a rather elaborate analysis is needed to treat the magnetic field perturbations. Moreover, a preliminary theoretical analysis led Wu *et al.*⁶ to conclude that because of strong Landau damping by thermal ions, ion-ion instabilities play little role in energy dissipation for strong shocks traveling through plasmas in space.

In Sec. 1 below we investigate the stability of an ion beam in a typical interstellar plasma; the ion-ion instabilities

are found to be important in spite of Landau damping if the perturbations of the magnetic field are treated correctly. The theory successfully describes the spectrum of the excited plasma waves and their time evolution deduced from measurements carried out in the joint Soviet-Czech "Intershok" program on board the "Prognoz-10-Interkosmos" satellite launched on 26 April 1985. The measurements are described in Sec. 2 and discussed further in Sec. 3.

1. EXCITATION OF LOWER-HYBRID OSCILLATIONS BY A BEAM OF REFLECTED IONS: THEORY

We thus start with the assumption that the primary source of free energy in strong shock waves is the motion of the reflected ions relative to the main plasma stream. Collisionless dissipation of energy in such shocks must therefore be associated with the growth of ion-ion two-stream instabilities.

We further assume that the solar wind plasma is nearly isothermal, so that ion-sound waves are not likely to be excited by the ion beam. We therefore consider only oscillations with frequencies and wave numbers in the interval

$$\omega_{ce} \gg \omega \gg \omega_{ci}, \quad k_{\perp} \rho_i \gg 1 \gg k_{\perp} \rho_e, \quad (1)$$

where ω is the wave frequency, k_{\perp} is the component of the wave vector normal to the magnetic field B , $\omega_{ej} = e_j B / m_j c$ is the cyclotron frequency for particles of species j (with charge e_j , mass m_j , and temperature T_j), and $v_{Tj} = (T_j / m_j)^{1/2}$ and $\rho_j = v_{Tj} / \omega_{ej}$ are the thermal velocity and Larmor frequencies. In a plasma at a finite pressure ($\beta_e \gtrsim 1$), the perturbation of the magnetic field at sub-lower-hybrid frequencies must be considered, while at higher frequencies one must allow for finite Larmor radius of the electrons.

We choose the coordinate axes so that the unperturbed magnetic field B_0 lies along the z axis and the wave vector is in the x, z plane. The space-time dependence of the oscillating electric and magnetic fields is then given by

$$E_x(\mathbf{r}, t) = E_{ix} \exp(-i\omega t + ik_x x + ik_z z). \quad (2)$$

To calculate the electric currents in the Maxwell equations, we must employ the kinetic description. The first-order solution f_{je} of the kinetic equation for the electron distribution function can be expressed as an integral over the unperturbed particle trajectories (see, e.g., Ref. 7)

$$f_{je}(\mathbf{r}, \mathbf{v}, t) = \frac{e}{m_e} \int_{-\infty}^t dt' \left\{ \mathbf{E}_1 + \frac{1}{c} [\mathbf{v}(t') \mathbf{B}_1] \right\} \times \frac{\partial f_{0e}}{\partial \mathbf{v}} \exp[-i\omega t' + i\mathbf{k}\mathbf{r}(t')]. \quad (3)$$

To calculate the trajectories it suffices to analyze the cyclotron rotation for free motion parallel to the magnetic field, i.e.,

$$\begin{aligned} z(t) &= z(0) + v_z t, \\ x(t) &= x(0) + (v_{\perp} / \omega_{ce}) [\cos(\theta - \omega_{ce} t) - \cos \theta], \\ v_x(t) &= v_{\perp} \sin(\theta - \omega_{ce} t), \quad v_y(t) = -v_{\perp} \cos(\theta - \omega_{ce} t), \end{aligned} \quad (4)$$

where θ is the cyclotron rotation phase. The integral over the

trajectories is readily evaluated by using the Bessel function expansion

$$e^{it \cos \theta} = \sum_{n=-\infty}^{+\infty} J_n(\xi) e^{in(\pi/2 - \theta)} \quad (5)$$

which implies the identities

$$\begin{aligned} v_x(t) \exp[ik_x x(t)] &= \exp \left[ik_x \left(x + \frac{v_y}{\omega_{ce}} \right) \right] \\ &\times \sum_{n=-\infty}^{+\infty} \frac{n \omega_{ce}}{k_x} J_n(\xi) \exp \left[in \left(\frac{\pi}{2} - \theta + \omega_{ce} t \right) \right], \\ v_y(t) \exp[ik_x x(t)] &= \exp \left[ik_x \left(x + \frac{v_y}{\omega_{ce}} \right) \right] \sum_{n=-\infty}^{+\infty} \\ &\times \frac{i \omega_{ce}}{k_x} \frac{\xi d}{d\xi} J_n(\xi) \exp \left[in \left(\frac{\pi}{2} - \theta + \omega_{ce} t \right) \right]. \end{aligned} \quad (6)$$

If we now use the fact that the thermal velocity distribution of the electrons is isotropic, we get the following correction to the lowest order distribution:

$$\begin{aligned} f_{je} &= \frac{ie}{m_e} \sum_{n=-\infty}^{+\infty} \frac{\exp \left[in \left(\frac{\pi}{2} - \theta \right) + ik_x v_y / \omega_{ce} \right]}{\omega - n \omega_{ce} - k_x v_x + i0} \\ &\times \exp(-i\omega t + ik_x x + ik_z z) \left\{ \left[\frac{n \omega_{ce} E_x}{k_x} J_n(\xi) \right. \right. \\ &\left. \left. + \frac{i \omega_{ce} E_y \xi}{k_x} \frac{dJ_n(\xi)}{d\xi} \right] \frac{\partial f_{0e}}{v_{\perp} \partial v_{\perp}} + E_x J_n(\xi) \frac{\partial f_{0e}}{\partial v_z} \right\}. \end{aligned} \quad (7)$$

If the influence of the unperturbed magnetic field on the ion motion is neglected, the corresponding first-order correction to the distribution function for the thermal ions ($j = i$) and for the ions in the beam ($j = b$) is

$$f_{ij} = -\frac{ie}{m_i} \left\{ \mathbf{E}_1 + \frac{1}{c} [\mathbf{v} \mathbf{B}_1] \right\} \frac{\partial f_{0i}}{\partial \mathbf{v}} (\omega - k_x v_x - k_z v_z + i0)^{-1}, \quad j = i, b. \quad (8)$$

Due to the strong Landau damping by the electrons, only waves traveling nearly perpendicular to the magnetic field can be excited in the plasma ($k_x \lesssim \omega / v_{Te} \ll k_{\perp}$). We can neglect the thermal motion of the electrons and ions along the magnetic field, and also the magnetic field B_y induced by the longitudinal electron current j_z . The Maxwell equations

$$k_x E_y = \omega B_z / c, \quad (9)$$

$$k_x B_x + k_z B_z = 0, \quad (10)$$

$$ik_x B_x - ik_z B_z = 4\pi j_y / c \quad (11)$$

relate the remaining field components; here most of the contribution to the electric current j_y comes from the electrons and ions in the beam, i.e.,

$$j_y = \sum_{j=e,b} e_j \int v_y f_{ij} d\mathbf{v}. \quad (12)$$

Together with Eqs. (9)–(12), the explicit expressions (7), (8) for the perturbations of the distribution functions give

$$\frac{\omega}{k_x c} B_z = E_y = \frac{i\omega E_x}{\omega_{ce}} \left\{ \frac{\omega_{pe}^2}{k_x^2 c^2} F_0' - \frac{i\omega_{pi}^2 \omega_{ce} V_{by}}{k_x^2 c^2 n_0} \right. \\ \times \int \frac{(\partial f_b / \partial v_x) dv}{\omega - k_x v_x + i0} \left. \right\} \\ \times \left\{ 1 - \beta_e F_0' - \frac{\omega_{pi}^2 k_x V_{by}^2}{k_x^2 c^2 n_0} \int \frac{(\partial f_b / \partial v_x) dv}{\omega - k_x v_x + i0} \right\}^{-1}, \quad (13)$$

where

$$F_0(\alpha) = e^{-\alpha} I_0(\alpha), \quad \alpha = k_x^2 \rho_e^2, \quad F_0' = dF_0(\alpha)/d\alpha,$$

and $I_0(\alpha)$ is a modified Bessel function. In evaluating the current of the ions in the beam we have assumed a distribution function of the form

$$f_b(v) = n_b \left(\frac{m_i}{2\pi T_b} \right)^{3/2} \exp \left[-\frac{m_i (v - V_b)^2}{2T_b} \right]. \quad (14)$$

The dispersion equation for the oscillations can be derived from the equation of continuity for the current, which follows from the Maxwell equations by neglecting the displacement currents:

$$\operatorname{div} j = 0. \quad (15)$$

Here we must include the contributions from both the beam and the thermal ions to the components j_x of the current; we get the result

$$\frac{\omega_{pe}^2}{\omega_{ce}^2} \frac{1 - F_0}{\alpha} + \omega_{pi}^2 F_0'^2 \left\{ k_x^2 V_A^2 (1 - \beta_e F_0') - \frac{\omega_{ce}^2 V_{by}^2}{n_0} \int \frac{k_x (\partial f_b / \partial v_x) dv}{\omega - k_x v_x + i0} \right\}^{-1} \\ + \sum_{j=i,b} \frac{\omega_{pi}^2}{n_0 k_x^2} \int \frac{k_x (\partial f_j / \partial v_x) dv}{\omega - k_x v_x + i0} = 0, \quad (16)$$

where $V_A = B / (4\pi n_0 m_i)^{1/2}$ is the Alfvén velocity.

We first analyze the solution of this dispersion equation when no ion beam is present ($n_b = 0$) and limit ourselves to the most interesting case $\beta_e \approx 1 - 3$, which is typical for solar wind. The two characteristic lengths—the cyclotron radius ρ_e of the thermal electrons and the skin length c/ω_{pe} —

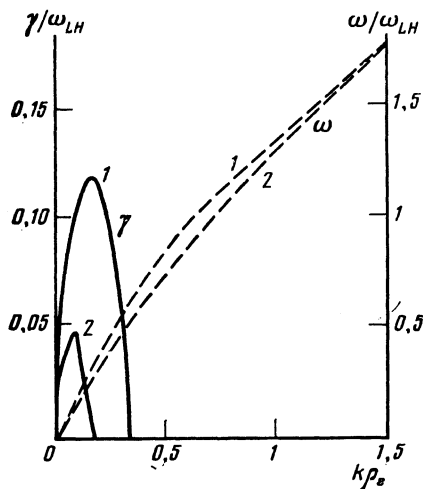


FIG. 1. Frequency ω and growth rate γ of the oscillations vs wave number k_{\perp} for $\beta_e = 1$ (curves 1) and $\beta_e = 4$ (curves 2).

are then comparable in order of magnitude. In the long-wave limit ($k_{\perp} \rho_e \approx k_{\perp} c/\omega_{pe} \ll 1$), the dispersion equation (16) describes magnetoacoustic waves propagating with phase velocity¹⁾ $V_j = V_A (1 + \beta_e)^{1/2}$. In the short-wave limit $k_{\perp} \rho_e \approx k_{\perp} c/\omega_{pe} \gg 1$, the waves are electrostatic ion-sound plasma oscillations, i.e., $\omega = k_{\perp} c_s$ (Fig. 1). Since the solar wind plasma is nearly isothermal ($T_e \approx 2T_i$), the ion-sound oscillations are strongly damped and cannot be sustained even by an intense beam of reflected ions.

We will show below that the growth rate for the beam instability remains small compared to the oscillation frequency, so that the dispersion equation (16) can be expanded in the small parameter $n_b/n_0 \ll 1$ to give

$$\frac{\omega_{pe}^2}{\omega_{ce}^2} \frac{1 - F_0}{\alpha} + \frac{\omega_{pi}^2 F_0'^2}{k_x^2 V_A^2 (1 - \beta_e F_0')} \\ + \frac{\omega_{pi}^2}{k_x^2 n_0} \int \frac{k_x (\partial f_b / \partial v_x) dv}{\omega - k_x v_x + i0} \\ + \frac{\omega_{pi}^2}{k_x^2 n_0} \left[1 + \frac{\omega_{ce}^2 V_{by}^2 F_0'^2}{k_x^2 V_A^4 (1 - \beta_e F_0')^2} \right] \\ \times \int \frac{k_x (\partial f_b / \partial v_x) dv}{\omega - k_x v_x + i0} = 0. \quad (17)$$

Here the second term in the factor in square brackets multiplying the integral in the last term is nonzero only if one allows for the electromagnetic nature of the oscillations (in particular, for the work done by the beam in the induced field E_y of the wave). Because the ratio m_e/m_i is small, one usually neglects the influence of the induced electric field on the ion oscillations in the wave (see, e.g., Refs. 6 and 7). However, we will show that for a supersonic ion beam ($V_{by} \gg V_j$), the induced field may pump magnetoacoustic oscillations at very long wavelengths which would otherwise be strongly damped in a plasma with $\beta_e \approx 1-3$ even when an ion beam is present.⁶ The growth rate for the kinetic instability of the ion beam and the frequency of the oscillations follow from the dispersion equation (17):

$$\gamma_k = \frac{\pi^{1/2} \omega_k^3}{k^2 c_s^2} \left\{ \frac{n_b T_e}{2n_0 T_b} \left[1 + \frac{m_e V_{by}^2 c_s^2 F_0'^2}{m_i \alpha V_A^4 (1 - \beta_e F_0')^2} \right] e^{-1/2} - \frac{\omega_k}{k c_s} \left(\frac{T_e}{2T_i} \right)^{3/2} \exp \left(-\frac{\omega_k^2 T_e}{2k^2 c_s^2 T_i} \right) \right\}, \quad (18)$$

$$\omega_k = \omega_{LH} \alpha^{1/2} [1 - F_0 + \beta_e F_0'^2 / 2(1 - \beta_e F_0')]^{-1/2}. \quad (19)$$

Here we have recalled that the ion beam oscillations grow most rapidly if the beam velocity and the phase velocity of the waves satisfy

$$(\omega_k - k_x V_{bx}) / k_x (T_b/m_i)^{1/2} \approx 1. \quad (20)$$

We see that the instability growth rate increases with the wavelength of the oscillations. However, expression (19) breaks down in the extreme long-wave limit, i.e., when $\gamma_1 > k_{\perp} v_{Tb}$, in which case the thermal spread of the beam can be neglected altogether and one must use the alternative expression

$$\gamma_k = \frac{\sqrt{3}}{2} \left(\frac{n_b m_e V_{by}^2}{n_0 m_i V_j^2} \right)^{1/2} \left(\frac{k_{\perp} V_j}{\omega_{LH}} \right)^{1/2} \omega_{LH} > k_{\perp} v_{Tb}. \quad (21)$$

for the growth rate. By comparing (19) and (21) we can estimate the maximum growth rate for the beam instability and the corresponding oscillation frequency:

$$\begin{aligned} \gamma_{\max} &\approx \left(\frac{n_b V_b v^2}{n_0 V_j^2} \right)^{1/2} \left(\frac{V_j}{v_{Tb}} \right)^{1/2} \omega_{ci}, \\ \omega_{\max} &= \left(\frac{n_b V_b v^2}{n_0 V_j^2} \right)^{1/2} \left(\frac{V_j}{v_{Tb}} \right)^{1/2} \omega_{ci}. \end{aligned} \quad (22)$$

Figure 1 shows how the growth rate depends on the wave number for typical magnetoacoustic Mach numbers $M = u_{sw}/V_A (1 + \beta_e + \beta_i)^{1/2} \approx 5$, beam velocity $V_b \approx 1.7 u_{sw}$, density $n_b = 0.25 n_0$, and temperature $T_b = T_i$ for two values $\beta_e = 2\beta_i = 1$ and $\beta_e = 2\beta_i = 4$. We see that γ drops as β increases, and the frequency of the fastest-growing mode also drops. The same behavior is observed if the thermal spread of the particle velocities in the beam increases as the beam relaxes quasilinearly under the influence of the growing oscillations.

We note that when a reflected ion beam is present, the electromagnetic nature of the long-wave magnetoacoustic oscillations can destabilize the plasma only if the velocity distribution is of the form (14). Because the velocity distribution of the reflected ions relaxes quasilinearly and the cyclotron phases of the ions become mixed behind the shock wave, we expect that the distribution of the reflected ions will take on the form of a "fuzzy ring" in velocity space, i.e.,

$$f_b(v_{\perp}) = \frac{n_b m_i}{\pi T_b} \exp \left[- \frac{m_i (v_{\perp}^2 - V_b^2)}{2 T_b} \right]. \quad (23)$$

The situation here is different because now the solenoidal fields effectively suppress the growth of the long-wave magnetoacoustic oscillations.⁸ If we recall that the ion temperature becomes greater than the electron temperature behind a strong shock wave, we conclude that the oscillations must be damped at some distance from the front.

2. MEASUREMENT OF THE LOWER-HYBRID SPECTRUM AND ITS DYNAMICS IN A BOW SHOCK

In this section we discuss measurements of the low-frequency fluctuations (0.5–20 Hz) in the electric and magnetic fields at the wavefront of an intense, nearly perpendicular

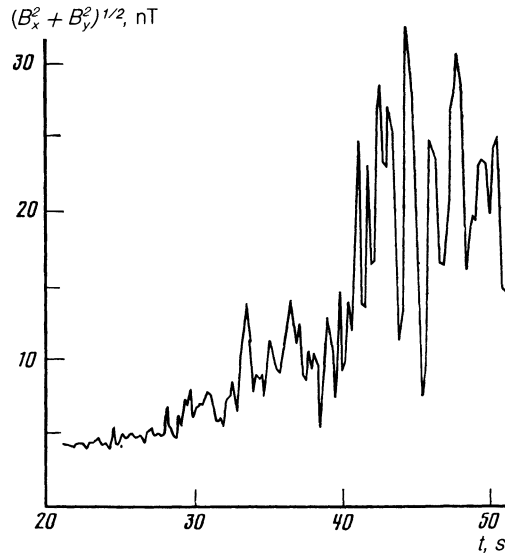


FIG. 2. Profile of the magnetic field $B = (B_x^2 + B_y^2)^{1/2}$ near the shock wave front.

bow shock. The data were recorded in the "BUDVAR" experiments on board the "Prognoz-10-Interkosmos" satellite, which was launched into a high-apogee orbit about the earth on 26 April 1985. The electric field oscillations were measured by the double floating probe technique, in which a dipole constructed from two spherical probes of length 1.85 m was mounted at one end of a 5-m-long bar. The oscillations in the magnetic field were measured by a two-component ferromagnetic magnetometer probe whose sensor was located at the other end of the bar. The satellite rotated at a rate of $3^\circ/\text{s}$ about an axis coinciding to within 5° with the direction to the sun.

Two components of the magnetic field were measured, one along the rotation axis of the satellite and the other perpendicular to it. The electric dipole was aligned normal to the axis of rotation and to the transverse magnetic field component. The sensitivities of the electric field receiver and two magnetic sensors were 0.5 mV/m and 0.1 nT, respectively. The data were transmitted directly to earth every 20 ms (50 Hz) and were mutually synchronized to better than 10 ms.

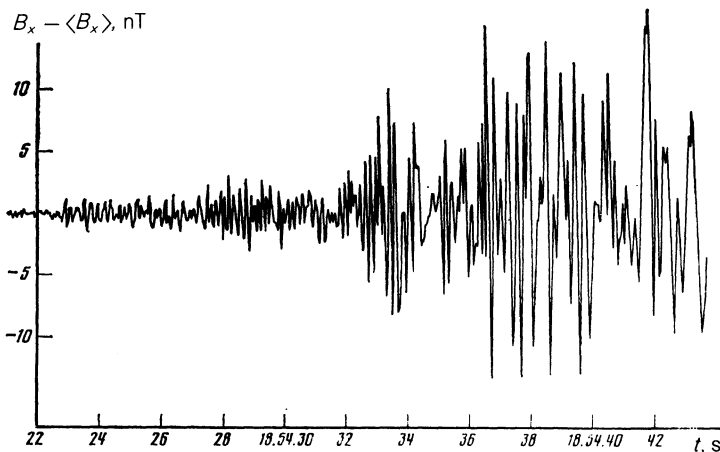


FIG. 3. Waveform of the oscillations in the x-component of the magnetic field.

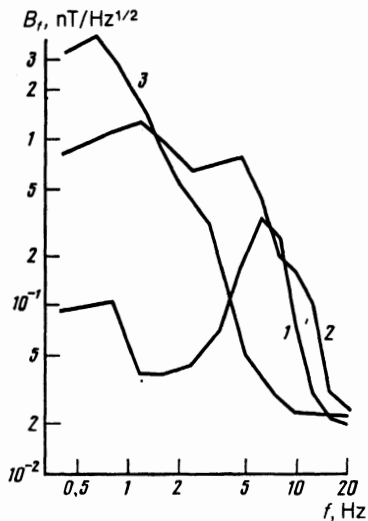


FIG. 4. Three successive spectra for the magnetic field oscillations obtained by Fourier-analyzing the waveform in Fig. 3. Traces 1, 2, and 3 correspond to the start of the precursor, the wavefront itself, and the wake, respectively.

Figure 2 shows the measured data for the two magnetic field components when the satellite crossed the earth's bow shock on 11 May 1985. The values were averaged over time intervals $\Delta t = 0.2$ s. The vertical axis plots the quantity $B_x^2 + B_y^2$, where the components B_x and B_y lie along and normal to the axis of rotation. The values $(B_x^2 + B_y^2)^{1/2}$ give a good lower bound for the magnitude of the magnetic field and serve to accurately identify the basic sequence of events when the shock wave was crossed. In the (unshown) portion of Fig. 2 to the left of time $t = 18:54:23$, the satellite was located in undisturbed solar wind. An increase in the magnetic field was then recorded for $18:54:23 < t < 18:54:41$, and abrupt fluctuations were noted; this stage may be identified as the "foot" of the shock wave. Such shock feet are familiar in laboratory experiments⁹ at high Mach numbers $M \gtrsim 3$ and are due to deceleration of the plasma flow in the self-consistent electric field (including the reflected ions); this deceleration is accompanied by plasma compression and enhancement of the magnetic field. The latter causes the forward-reflected ions to gyrate, and the size of the foot in the magnetic field profile is therefore comparable in order of magnitude to the Larmor radius of the reflected ions. During the third stage $18:54:41 < t < 18:54:43$ the field increased abruptly and large fluctuations were present. This stage may be identified with the shock wavefront proper. Finally, the plasma behind the shock relaxed for $t > 18:54:43$. In addition to the rise in the magnetic field, the foot is characterized by quasiperiodic oscillations both in the electric field and in the magnetic field components B_x , B_y . Figure 3 shows the fluctuating component for B_x ; oscillations of amplitude ≈ 1 nT and frequency 4–6 Hz were observed starting at 18:54:23, and their amplitude increased as the shock front was approached. The oscillations began to exhibit a low-frequency modulation starting at 18:54:28, and the modulation increased with the oscillation amplitude (12–15 nT). The frequency of the oscillations decreased as the front was ap-

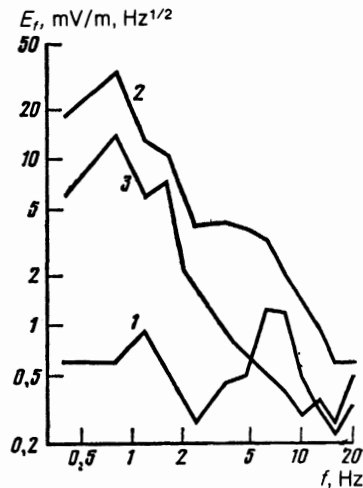


FIG. 5. Successive spectra for the electric field (the traces are labeled as in Fig. 4).

proached, and oscillations of frequency ≤ 1 Hz were observed for roughly 2 min after the shock was crossed at 18:54:42.

The time behavior of the oscillation spectrum is illustrated in Figs. 4 and 5, which show three successive spectra recorded for B_x (along the satellite rotation axis, i.e., toward the sun) and E_z (normal to the rotation axis). Spectrum 1 was recorded 10 s before the front was crossed; it reveals a distinct energy peak at 4–6 Hz. This peak lies at 0.7 Hz in traces 2 and 3 at and behind the front, respectively (the front itself was identified with the sudden jump in the strength of the magnetic field).

3. DISCUSSION

Before we can quantitatively compare the extremely low-frequency plasma-wave measurements in a bow shock wave with the predictions of the theory of ion beam instability developed above, we must estimate the basic parameters of the shock wave and the hydrodynamic parameters of the undisturbed solar wind preceding it. The ions (mostly protons) in the solar wind were recorded by "Monitor" and "BIFRAM" detectors on board the "Prognoz-10-Interkosmos" satellite. The results were: density $n_0 = 15 \text{ cm}^{-3}$, velocity $u_{sw} = 350 \text{ km/s}$, and temperature $T_p = 4 \text{ eV}$ for the protons in the solar wind. The unperturbed field $B_0 = 4.5 \text{ nT}$ was recorded by a magnetometer in the system used to detect the plasma waves (Fig. 2). In the subsequent estimates we assume values $T_e \approx 10 \text{ eV}$ typical for solar wind. Since bow shocks travel much less rapidly than the solar wind, the Mach number at the shock wave can be found from the relation

$$M = u_{sw} / V_A (1 + \beta_e + \beta_i)^{1/2} \approx 5.9, \quad (24)$$

where $\beta_i \approx 1.2$ and $B_e \approx 3$.

The angle θ_{Bn} between the normal to the shock front and the magnetic field lines is an important parameter; it is usually calculated by assuming that the component of the magnetic field normal to the front is the same on both

sides.¹⁰ The resulting value $\theta_{Bn} \approx 65^\circ$ agrees closely with the angle $\theta_{Bn} \approx 70^\circ$ deduced from the coordinates of the point at which the satellite crossed the front by using the mean-square model for the profile of earth bow shocks.¹¹

Strictly speaking, simultaneous measurements from two satellites are needed in order to find the shock wave velocity u_{sh} . However, u_{sh} can be estimated if we assume that the ions reflected by the front are responsible for exciting the lower-hybrid magnetoacoustic oscillations as well as for compressing the plasma and the interplanetary magnetic field frozen into it (Fig. 2). The width of the foot and the diameter of the region in which the waves are excited are then determined by the Larmor radius of the reflected ions, by the angles between the normal to the front and the magnetic field, and also by the plasma velocity.¹² If we use the plasma and shock wave parameters cited above and assume a foot of length $\Delta t = 18$ s (from the start of the foot to the jump in the magnetic field at the front), we get the estimate $u_{sh} = 10$ km/s for the shock wave velocity relative to the satellite.

We can now use these plasma and shock wave parameters to compare the measured results with the theory. If we take typical values $n_b = 0.25n_0$, $V_b \approx 1.7u_{sw}$ (Ref. 1) for the density and velocity of the reflected ions and use the parameter values for undisturbed solar wind, Eqs. (22) give the numerical estimate $\gamma_{\max} = 3.3 \text{ s}^{-1}$ for the growth rate and $f_{\max} = 0.8 \text{ Hz}$ for the oscillation frequency in a coordinate system moving with the plasma. The oscillation frequency in a system moving with the satellite is considerably higher due to the Doppler effect (the oscillations are transported together with the plasma at the solar wind velocity u_{sw}): $f_D = fu_{sw}/V_f = 5.5 \text{ Hz}$, and the initial spectrum (trace 1, Figs. 4, 5) does indeed have a peak at this frequency. The frequency then drops rapidly to $f_D \approx 0.7 \text{ Hz}$ because the velocities of the reflected ions relax—as the thermal velocity spread of the ions increases as a result of the oscillations, the frequency of the fastest-growing oscillations decreases in accordance with (20). We note that the oscillations propagating normal to the beam in the coordinate system moving with the plasma are in resonance with the beam. The energy distribution of the beam therefore relaxes more slowly than the angular distribution, in agreement with the measurements.⁴

According to Fig. 3, the typical growth time for the oscillations measured by the satellite was $\tau = 10$ s, so that we have the estimate $\gamma \approx u_{sw}/u_{sh} \tau = 4 \text{ s}^{-1}$ for the growth rate, in good agreement with the estimate given above. We note that this estimate is quite crude due to the error in estimating u_{sh} from measurements obtained from a single satellite. The ratio of the measured fluctuations $B_f \approx 0.3 \text{ nT} \cdot \text{Hz}^{1/2}$ and $E_f \approx 1 \text{ mV/m} \cdot \text{Hz}^{1/2}$ in the magnetic and electric fields at the start of the foot agrees closely with the theoretical value (13) $B_f/E_f = f_{pi}/f \approx 500$ calculated using the parameter values for unperturbed solar wind. The oscillation amplitude can also be estimated by assuming that oscillations with a well-defined frequency stop growing when the resonant

ions in the beam are trapped in the electric field of the wave, i.e., when

$$(eE/m_i)^{1/2} \approx (\omega - k_x V_{bx})/k \approx v_{Tb}. \quad (25)$$

If we assume that $T_i \approx T_e$ we get the value $E \approx 1 \text{ mV/m}$, in good agreement with the measurements.

Finally, the quasilinear relaxation theory gives the estimate

$$\tau_{QL}^{-1} \approx (e^2/m_i \Delta V_b^2 f_{\max}) \int E_f^2 df \quad (26)$$

for the characteristic relaxation time of the reflected ion beam behind the shock wave front (the ions are deflected into this region by the magnetic field). For the oscillation amplitudes $E_f \approx 10 \text{ mV/m} \cdot \text{Hz}^{1/2}$ measured behind the front, the velocity scatter in the beam reaches $\Delta V_b \approx V_b$ (at which growth stops) during a time $\tau_{QL} \approx 10$ s, i.e., the oscillations extend out a distance of $L \approx 10^3 \text{ km}$ from the front when the plasma velocity in the wake is $u \approx 100 \text{ km/s}$; the satellite travels this distance during a time $L/u_{sh} \approx 10^2 \text{ s}$, again in agreement with our measurements.

The theoretical estimates thus agree with measurements made on board the "Prognoz-10-Interkosmos" satellite in the USSR-Czech "Intershok" program. This demonstrates convincingly that the magnetoacoustic oscillations at low-hybrid frequencies are excited by a beam of ions reflected from the shock wave.

We thank P. Triska, Ya. Voita, V. E. Korepanov, S. A. Romanov, and S. P. Savin for help in setting up the wave experiment in the "Intershok" project, and O. L. Vašberg and G. N. Zastenker for making available to us the solar wind measurements carried out in the same plasma experiment.

¹⁾ Because these oscillations become whistlers as the longitudinal component k_z of the wave vector increases, they are often referred to as whistlers even when $k_z \rightarrow 0$.

¹⁾ N. Sckopke, G. Paschman, S. I. Bame, J. T. Gosling, and C. T. Russell, *J. Geophys. Res.* **88**, 6121 (1983).

²⁾ R. Z. Sagdeev, *Zh. Tekh. Fiz.* **31**, 1185 (1961) [*Sov. Phys. Tech. Phys.* **31**, 867 (1961)].

³⁾ M. M. Leroy, D. Winske, C. C. Goodrich, C. S. Wu, and K. Papadopoulos, *J. Geophys. Res.* **87**, 5081 (1982).

⁴⁾ G. Paschman, N. Sckopke, I. Papamastorakis, *et al.*, *J. Geophys. Res.* **86**, 4355 (1981).

⁵⁾ O. L. Vašberg, A. A. Galeev, S. I. Klimos, *et al.*, *Pis'ma Zh. Eksp. Teor. Fiz.* **35**, 25 (1982) [*JETP Lett.* **35**, 30 (1982)].

⁶⁾ C. S. Wu, D. Winske, Y. M. Zhou, *et al.*, *Space Sci. Rev.* **37**, 63 (1984).

⁷⁾ A. B. Mikhailovskii, *Teoriya Plazmennykh Neustoichivostei* (Theory of Plasma Instabilities), Vol. 1, Atomizdat, Moscow (1975), pp. 227, 263.

⁸⁾ A. A. Galeev, in: *Proc. Spring College on Plasma Physics*, ICTP, Trieste, May 1985, Lecture SMR/150-11.

⁹⁾ R. Ch. Kurtmullaev, Yu. E. Nesterikhin, V. I. Pilsky, and R. Z. Sagdeev, in: *Plasma Phys. and Contr. Nucl. Fusion Res.*, Vol. 1, IAEA, Vienna (1966), p. 367.

¹⁰⁾ L. D. Landau and E. M. Lifshitz, *Electrodynamics of Continuous Media*, 2nd ed., Pergamon (1984).

¹¹⁾ V. Formisano, *Planet. Space Sci.* **27**, 1151 (1979).

¹²⁾ W. A. Livesey, C. T. Russell, and C. F. Kennel, *J. Geophys. Res.* **89**, 6824 (1984).

Translated by A. Mason